Hydrology Research

Hydrology Research Vol 55 No 11, 1143 doi: 10.2166/nh.2024.066

Ensemble modeling of the hydrological impacts of climate change: A case study of the Baro River sub-basin, Ethiopia

Bekele Terefe Gebisa[a] and Wakjira Takala Dibaba[b,*]

[a] Department of Hydraulic and Water Resources Engineering, Bule Hora University, Bule Hora, Ethiopia
[b] Department of Hydraulic and Water Resources Engineering, Jimma University, Jimma, Ethiopia
*Corresponding author. E-mail: wakjira.takala@ju.edu.et

WTD, 0000-0002-9359-2142

ABSTRACT

Given the Baro River basin's high climatic variability and frequent flooding, climate change is expected to exacerbate the existing issues in the region. Three best-performing climate models from Coupled Model Intercomparison Project phase 6 (CMIP6) were used to examine the potential impact of climate change on the hydrology of the Baro River sub-basin. The ensemble of the climate models were bias-corrected for the climate change analysis and a calibrated and validated Soil and Water Assessment Tool (SWAT) model was used to examine the impact of the climate changes under two shared socioeconomic pathways (SSP2-4.5 and SSP5-8.5) in the future (2031–2060). The climate change scenarios projected an increase in precipitation and temperature under all scenarios. Consequently, annual increase in surface runoff, water yield, and potential evapotranspiration (PET) was reported by 30.33% (44.67%), 6% (18.1%,), and 4.49% (6.63%) and decline in groundwater by 13.17% (2.64%) under SSP2-4.5 (SSP5-8.5), respectively. The rise in temperature and PET could be responsible for the decline in groundwater, while the projected increase in precipitation is expected to enhance surface runoff, perhaps leading to flooding. This requires an improved water management policy that involves all sectors and takes into account the equity for different users.

Key words: Baro River sub-basin, climate change, CMIP6, hydrology

HIGHLIGHTS

- Climate change scenarios projected an increase in precipitation and temperature.
- Annual surface runoff and water yield are projected to increase under the climate change.
- Annual groundwater is projected to decline due to the climate change.
- The rise in temperature and PET could be responsible for the decline in groundwater.
- The increasing precipitation projected an increase of surface runoff.

GRAPHICAL ABSTRACT

Spatial Distribution of Surface Runoff and Water Yield under base line (1985-2014) and future (2030-2060) climate scenario

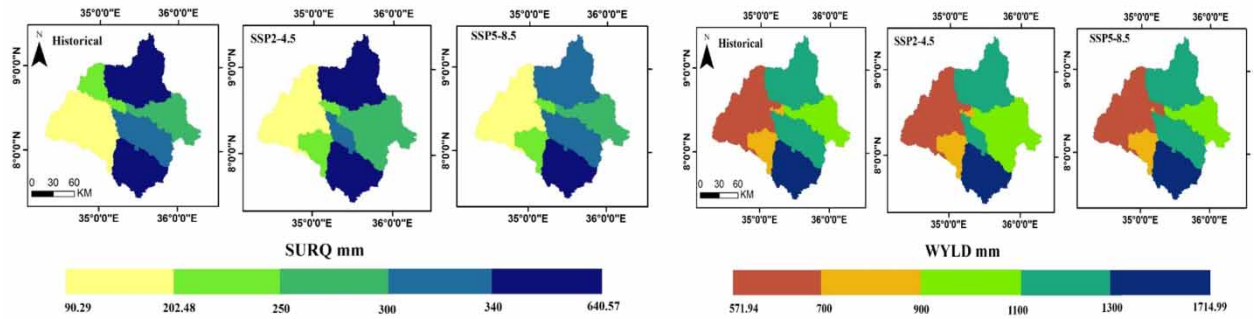

Spatial Distribution of Ground water and Evapotranspiration under base line (1985-2014) and future (2030-2060) climate scenario

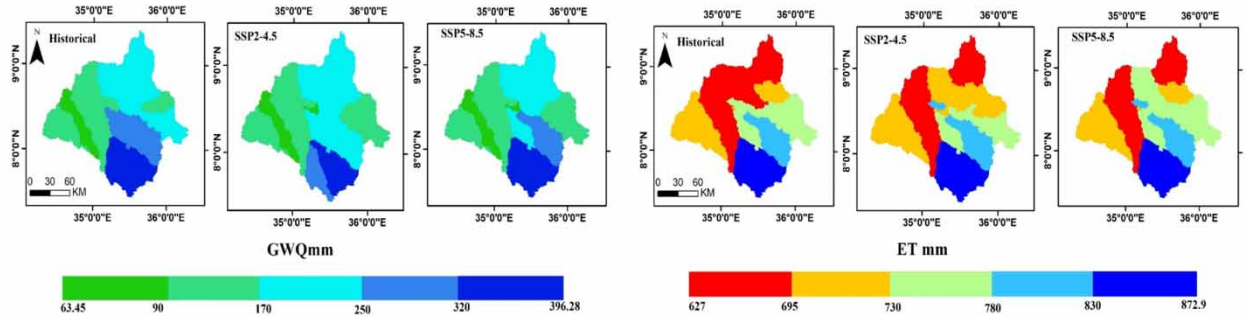

1. INTRODUCTION

The Earth's climate has been experiencing a warming trend over the past 50 years (IPCC 2013), and this warming has had a considerable impact on the availability of water, human health, and food security (Gelete *et al.* 2020). One of the most noticeable effects of climate change is the increase in the frequency and severity of floods and droughts, as well as alterations in water supplies brought on by changes in temperature, precipitation patterns, soil moisture, humidity, runoff, and other hydrological cycles (Worku *et al.* 2021). Elevated temperatures accelerate the global water cycle, increasing the likelihood of extreme hydrological events and changing water resources are distributed globally at various scales (Chen *et al.* 2015). These hydrological changes have far-reaching consequences on many aspects of human well-being such as the availability of water, agricultural productivity, and the production of energy.

Recently, the impacts of climate change on hydrological processes and the availability of water at various spatial scales have been the subject of several research works. According to Coulibaly *et al.* (2018), the impact of climate change on water resources in the transboundary watershed of West Africa is projected to decline in the 21st century as a result of decreasing precipitation. In their 2018 study, Bodian *et al.* (2018) looked at the effects of climate change on the two main river basins in the Senegal, West Africa. The findings from multiple models revealed a decline in annual streamflow under both RCP4.5 and RCP8.5 scenarios. In the Blue Nile Basin of Ethiopia, it is predicted that precipitation will increase by 7–48% and the streamflow is estimated to undergo an increase ranging from 21 to 97% (Roth *et al.* 2018). Likewise, Tigabu *et al.* (2021) investigated how climate change may affect different aspects of the water balance in the Ethiopian watershed of Lake Tana. The study reported a slight change in rainfall but a decline in the number of rainy days in the Tana sub-basin. Overall, the various impacts of the climate change can be linked to differences in geographical locations, climatic features of river basins and differences in emission scenarios used.

The way that different studies use simulations from climate models varies. Some studies used the outputs of regional climate models (RCMs) and global climate models (GCMs) directly (Beyene *et al.* 2010; Setegn *et al.* 2011). The output from a climate model, however, must first go through some sort of preprocessing to remove any biases that may be present

before being used directly for hydrological simulation (Haerter *et al.* 2011). Some studies have utilized bias-adjusted and downscaled climate model results before incorporating them into hydrological evaluations (Bodian *et al.* 2018; Galata *et al.* 2021). To improve the accuracy of their simulations, climate models should, therefore, undergo downscaling and bias correction before being used to evaluate hydrological implications (Pierce *et al.* 2015).

Ethiopia experienced climate-related hazards such as floods, droughts, intense rainfall, and heatwaves based on historical records. For example, the country experienced significant flood events resulting in the loss of life and damage to property in various regions during the years 1988, 1993, 1994, 1995, 1996, and 2006 (NMA 2007). Numerous studies have been carried out at the watershed and basin scales to determine how climate change may affect water resources. For example, Taye *et al.* (2018) used three global climate models (GCMs) from the Combined Inter-Model Comparison Project Phase 5 (CMIP5) to examine the impacts of climate change on water resources of the Awash Basin. The study found that there is an increase in water deficiency in all seasons due to the projected decrease in precipitation and increase in temperature. Chaemiso *et al.* (2016), on the other hand, projected an increase in surface runoff and total water yield for the 2030 and 2090s in the Omogibe River Basin, Ethiopia. The varying effects of climate change on water resources across basins highlight the significance of understanding the hydrological implications using appropriate climate change scenarios. Multiple studies have evaluated the Upper Blue Nile Basin's water resources and projected both positive and negative effects of climate change on the basin. For instance, Roth *et al.* (2018) used three models with the Soil and Water Assessment Tool (SWAT) hydrological model and reported an increase in precipitation and streamflow from the Blue Nile. Similarly, Wagena *et al.* (2016) reported an increase in mean annual flows for the Tana and Beles basins under climate change. On the contrary, the reduction in annual precipitation and increase in temperature reported on Jemma sub-basin of the Upper Blue Nile Basin projected a reduced surface runoff and water yield (Worku *et al.* 2021). Overall, it was observed that the hydrological process would vary as a result of the projected changes in temperature and precipitation. However, the degree of the prevailing change in temperature and precipitation determines how much has changed.

The Baro River sub-basin experiences significant climate variability, leading to frequent fluctuations in hydrological process due to the impacts of climate change (Muleta 2021; Mengistu *et al.* 2023). Both studies reported increasing temperature projections, however, precipitation projections have not shown a systematic increase or decrease (Muleta 2021) and Mengistu *et al.* (2020) reported a decrease in precipitation. Moreover, both studies lack up-to-date information on the current climate scenarios. For example, the climate change studies are developed based on the Special Report on Emission Scenario (SRES) based on A1B storyline (Muleta 2021) and RCP4.5 and RCP8.5 under CMIP5 (Mengistu *et al.* 2020). It is evident that the precipitation projections from the two studies show discrepancies for the same area. It will be difficult to understand the hydrological process of the Baro-Akobo River basin under such discrepancy. Therefore, comprehensive investigation is required to establish the projections of climate variables selecting the best-performing multi-model outputs. Especially, in areas with complex topography, a single model is not representative as precipitation is highly affected by orography. One way to reduce climate model discrepancies is by using multi-model GCMs with the most recent state-of-the-art climate models, properly evaluating the strengths and weaknesses of individual and ensemble models. Therefore, to completely understand how the basin's hydrology responds to various climate scenarios, it is necessary to simulate the Baro River sub-basin's hydrological processes using the most recent Coupled Model Intercomparison Project Phase 6 (CMIP6) developments.

In the Baro River sub-basin, rainfall projections show significant seasonal variation, with summer and autumn experiencing a significant increase and winter and spring seeing a decrease. An evident consequence of this fluctuation will be the likelihood of hydrologic extremes, such as drought and flooding, over the basin due to the significantly increased evapotranspiration (ET) (Muleta 2021). The livelihoods of most of the inhabitants are based on rain-fed agriculture and are often affected by climate change. This suggests that smallholder farmers' livelihoods would be significantly affected by climate change, and thorough climate impact assessments are needed to inform climate change adaptation strategies. In order to reduce the uncertainties associated with particular GCMs, this study used models that are considered atypical or least realistic within a specific study area as demonstrated in Gebisa *et al.* (2023). By utilizing spatial, seasonal, and multivariate statistics, Gebisa *et al.* (2023) employed the multi-mean ensemble to select representative models.

The significance of this study stems from its use of the advanced Phase 6 CMIP6 model for the Baro River sub-basin. Initially, the research carefully selected the top-ranked GCMs, as described by Gebisa *et al.* (2023). This combination of modeling approaches provides a thorough understanding of the hydrological dynamics in this specific region, deepening the study's findings. In view of the challenges caused by climate change in various regions, this study is especially important

because it provides a thorough examination of the hydrological components of the Baro River sub-basin. The assessment of climate change impacts on hydrological components at the watershed and sub-basin levels will provide valuable assistance to both governmental and non-governmental organizations engaged in watershed planning and management.

2. MATERIALS AD METHODS

2.1. Study area

The Baro River sub-basin, situated in the Baro-Akobo basin, has the distinction of being the area's main river in the region. It is a transboundary river that rises in Ethiopia's western highlands and eventually merges into the Nile River. Geographically, it is located in western Ethiopia, positioned between latitudes 5°40′ and 10°50′ N and longitudes 33°20′ and 36°20″ E (Figure 1). The river basin exhibits a diverse topography, with elevation ranges from 416 to 3,266 m at the lowest point.

The meteorological stations utilized in this study include the following nine locations: Alemteferi, Yubdo, Gimbi, Dambidollo, Bure, Uka, Gore, Masha, and Matuhospital. However, three stations have a poor temperature record with missing values of more than 10%. Therefore, only six stations are used for temperature (Alem Teferi, Gore, Masha, Matu Hospital, Yubdo, and Dambidollo), while all stations are used for precipitations. Detailed information on the meteorological stations, including latitude, longitude, and elevation, along with weather variable records, is presented in Table 1. Solar radiation, wind speed, and relative humidity data are available only at one station (Gore).

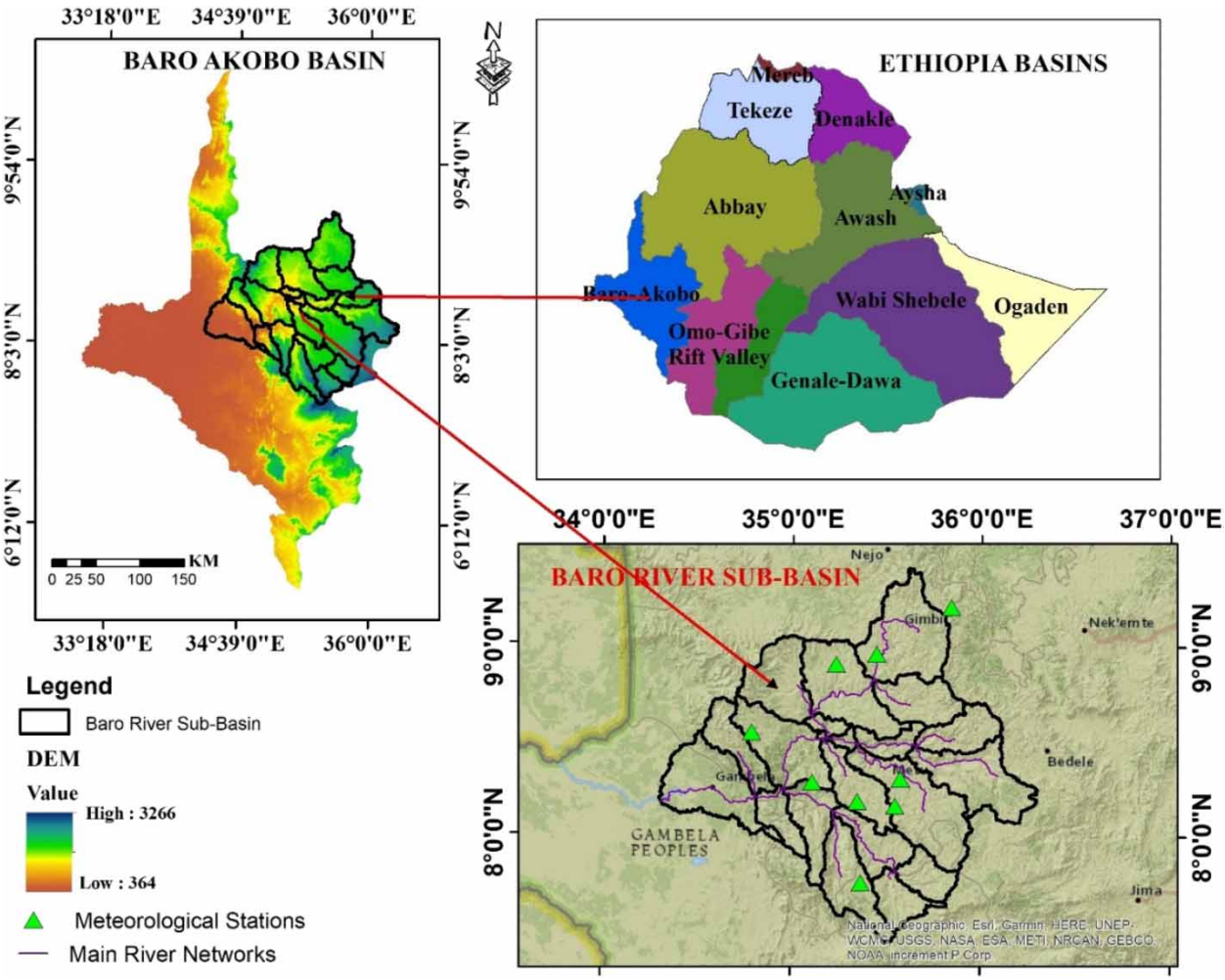

Figure 1 | Location of the study area.

Table 1 | Details of the meteorological stations used in this study

No.	Stations	Latitude	Longitude	Elevation	T_{max}	RH	T_{min}	SR	PCP	WS
1	Aemteferi	8.9	35.23	1,630	✓		✓		✓	
2	Bure	8.28	35.11	1,704					✓	
3	Gimbi	9.20	35.84	1,844					✓	
4	Gore	8.16	35.55	2,024	✓	✓	✓	✓	✓	✓
5	Masha	7.75	35.37	2,235	✓		✓		✓	
6	Matuhospital	8.29	35.58	1,702	✓		✓		✓	
7	Uka	8.18	35.35	1,667					✓	
8	Yubdo	8.95	35.45	1,550	✓		✓		✓	
9	Dembidollo	8.54	34.79	1,811	✓		✓		✓	

Note: ✓ denotes data availability.

SR, solar radiation; WS, wind speed; RH, relative humidity.

2.2. Data and methods

2.2.1. Digital elevation model

The topography of the watershed was established using the 30 × 30 m digital elevation model (DEM) in order to identify the watershed boundary, define the stream network, and generate sub-basins. Moreover, DEM facilitated the extraction of essential sub-basin parameters such as terrain slope length, slope gradient, stream network, slope classes, and channel lengths. The DEM data used in this study was obtained from the United States Geological Survey (USGS) at https://earthexplorer.usgs.gov/.

2.2.2. Land use/land cover

The land use/land cover (LULC) data of 2016 obtained from the Ministry of Agriculture and Ethiopian Mapping Agency show that Forest-Evergreen (FRSE) and Agricultural Land-Generic (AGRL) are the dominant LULC classes. FRSE and AGRL make up 61.6 and 29.5% of the total land area in the Baro River sub-basin, respectively. Figure 2 presents the different LULC classes in the study area.

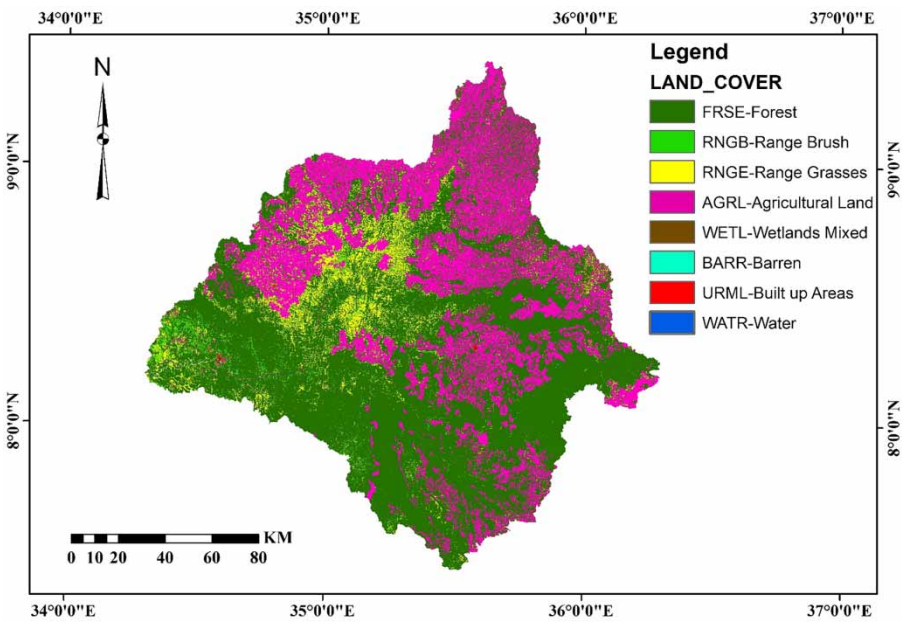

Figure 2 | LULC of the Baro River sub-basin.

2.2.3. Soil

Physical characteristics of each soil horizon have a significant impact on how water and air travel through the soil profile, which in turn affects how much water cycles through the hydrological response unit (HRU). These characteristics are used to determine the water budget, day-to-day runoff, and erosion of the soil profile. For this study, soil data provided by the Oromia Water Works Design and Supervision Enterprise (OWWDSE) were used. OWWDSE established soil attributes such as moisture content availability, hydraulic conductivity, bulk density, organic carbon content, texture, and chemical composition for distinct strata of each particular soil type. The different soil types in the study area are shown in Figure 3. The Humic Nitisols is the dominant soil type making up 67.38% of the total land area.

2.2.4. Hydrological data

Daily flow data are required to evaluate the performance of the SWAT model. The daily streamflow data of the Baro River sub-basin at the Gambella gauging station from 1985 to 2009 were collected from the Ministry of Water and Energy's Hydrology Department, and observed meteorological data were collected from the National Meteorological Agency (NMA) of Ethiopia from 1985 to 2014. The observed streamflow data were used for calibration and validation from 1990 to 2002 and 2003 to 2009, respectively, with a warm-up period of three years (1987–1989).

2.3. Climate change scenario and impact assessment

Following the evaluation of global climate models (GCMs), three models that exhibited superior performance were chosen (Gebisa *et al.* 2023). According to Gebisa *et al.* (2023), a detailed analysis of the GCMs evaluations revealed that the ensemble mean of three GCMs outperformed the individual GCMs and the ensemble of all GCMs. The authors downscaled the GCMs to better suit specific applications, selecting the best-performing model based on multi-evaluation criteria. Accordingly, GCMs used in this study are GFDL-CM4, INM-CM4-8, and INM-CM5-0 for precipitation and minimum temperature and CMCC-ESM2, MRI-ESM2-0, and INM-CM4-8 for maximum temperature under the SSP2-4.5 and SSP5-8.5. In this study, the hydrological responses of the basin to climate change impacts were modeled for the future period spanning 2031–2060, with the baseline period covering 1985–2014. While considering future scenarios, other weather variables like solar radiation, relative humidity, and wind speed in the historical period were maintained without alteration as changes in these variables might not have a substantial impact on the local hydrology compared to the precipitation and temperature (Arnell 2003; IPCC 2014).

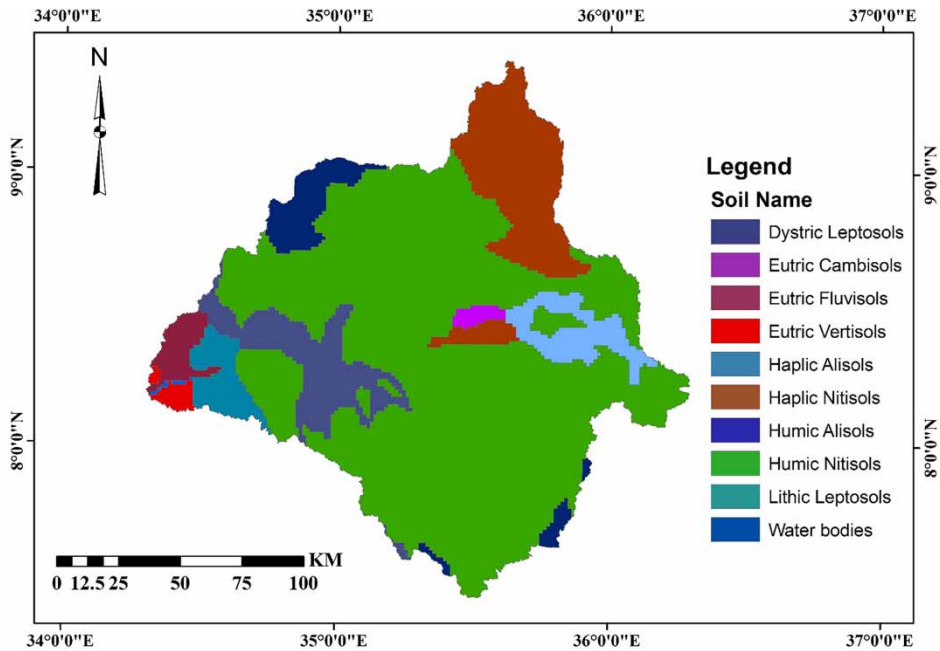

Figure 3 | Soil map of the Baro River sub-basin.

Moreover, baseline data for solar radiation, wind speed, and relative humidity are available only for limited time periods and from a few stations in Baro River sub-basin.

2.4. Bias correction

Despite the ensemble mean and individual GCMs' satisfactory performance, it was found that three of them showed clear biases. Therefore, it is essential to examine and reduce these biases before beginning a study on how climate change will affect hydrology. Linear scaling (LS) for precipitation and distribution mapping (DM) for temperature were used for bias correction in this study. More comprehensive information regarding the GCM models, downscaling method, and bias correction technique can be found in the work conducted by Gebisa *et al.* (2023).

2.5. Hydrological model

A continuous-time model called SWAT was developed in the early 1990s to assist water resource managers in estimating the impact of management and climate on water supplies and non-point source pollution in watersheds and major river basins (Arnold & Fohrer 2005). In typical SWAT modeling applications, basins are divided into sub-basins, which are further split into HRUs, homogeneous areas of dense soil, land use, and slopes (Neitsch *et al.* 2005). Furthermore, the SWAT model is capable of simulating important hydrological processes such as surface runoff, percolation, ET, infiltration, deep aquifer fluxes, channel routing, and shallow aquifer. The following water balance equation serves as the foundation for SWAT's simulation of the hydrologic cycle:

$$\mathrm{SW_t} = \mathrm{SW_o} + \left[\sum_{i=1}^{t} (R_{\mathrm{day}} - Q_{\mathrm{surf}} - \mathrm{Ea} - W_{\mathrm{seep}} - Q_{\mathrm{gw}})\right] \tag{1}$$

where $\mathrm{SW_t}$ is the soil's final soil water content (mm), $\mathrm{SW_o}$ is the initial soil water content on day i (mm), t is the time (days), R_{day} is the amount of precipitation on day i (mm), Q_{surf} is the amount of surface runoff on day i (mm), Ea is the amount of ET on day i (mm), W_{seep} is the amount of water entering the vadose and Q_{gw} is the amount of return flow on day i (mm) (Neitsch *et al.* 2005).

The SWAT model simulates surface runoff (SURQ) and peak runoff rates for each HRU by employing daily rainfall data and the curve number (CN) provided by the soil conservation service (SCS) (Neitsch *et al.* 2011). In this particular investigation, a customized SCS CN was employed to calculate the surface runoff:

$$Q_{\mathrm{surf}} = \frac{(R_{\mathrm{day}} - Ia)^2}{(R_{\mathrm{day}} - Ia + S)} \tag{2}$$

where Q_{surf} is the cumulative runoff or rainfall excess (mm H_2O), R_{day} is the rainfall depth for the day (mmH_2O), Ia is the initial abstraction (mmH_2O), and S is the retention parameter (H_2O).

SWAT utilizes three approaches to compute PET: the Penman–Monteith method, the Priestley–Taylor method, and the Hargreaves method (Neitsch *et al.* 2005). In this research paper, the Penman–Monteith technique is employed for estimating potential evapotranspiration (PET):

$$\lambda E = \frac{\Delta.(H_{\mathrm{net}} - G) + \rho_{\mathrm{air}}.Cp.[e^{\circ} - ez]/ra}{\Delta + \gamma.(1 + (rc/ra))} \tag{3}$$

where λE is the latent heat flux density, E is the depth rate evaporation, Δ is the slope of the saturation vapor pressure–temperature curve, H_{net} is the net radiation, ρ_{air} is the air density, Cp is the specific heat at constant pressure, e° is saturation vapor pressure, ez is the water vapor pressure of air, γ is the psychometric constant, rc is the plant canopy resistance, ra is the diffusion resistance of the air layer, and G is the heat flux density to ground.

The SWAT model's simulation of the hydrological process begins with the definition of watersheds and the construction of streamflow networks. Using a 30-m resolution DEM, the Baro River sub-basin was divided into 21 sub-basins, and a multiple HRU was established. Consequently, 309 HRUs were produced. With the input of weather data from five stations, the SWAT model setup was then prepared for the first simulation, which was utilized for model evaluation.

Assessment of the impact of climate change on water resources is made possible by coupling the SWAT hydrologic model with the global climate models (Saharia & Sarma 2018). The model's performance for the river basin was examined before looking at the results of the SWAT simulation. The parameters of SWAT model were calibrated and validated using historical data, and they were assumed extrapolative under future scenarios.

2.5.1. Sensitivity analysis, calibration, and validation

Finding the most important factors among the model parameters is essential for enhancing the calibration of the hydrological model in SWAT. Sensitivity analysis is essential in identifying the extremely sensitive variables that have a big effect on the flow process. For the SWAT, a number of calibration techniques have been developed with the SWAT Calibration and Uncertainty Program (SWAT-CUP), with Sequential Uncertainty Fitting 2 (SUFI-2) being the most extensively used. This calibration process incorporates a variety of objective functions to enhance the accuracy of the model (Sao *et al.* 2020).

The process of model calibration involves adjusting model parameters to align with observed data while allowing for a certain level of variability. To reduce uncertainty in calculating process parameters, a variety of strategies are used during calibration. Validation includes the comparison of model outcomes with an independent dataset, without making any additional adjustments to the parameter values. A warm-up period from 1987 to 1989, a calibration period from 1990 to 2002, and a validation period from 2003 to 2009 were used to evaluate the performance of the hydrological model.

To evaluate the model's effectiveness, various statistical methods were employed, for example the coefficient of determination (R^2), Nash–Sutcliffe efficiency (NSE), percent bias (PBIAS), and the ratio of root mean square error (RMSE) to the standard deviation of observations (RSR). The selection of these statistical approaches plays a crucial role in the evaluation process (Khatun *et al.* 2018):

$$R^2 = \frac{\sum_{i=0}^{n} [(Q_{\text{sim}} - \bar{Q}_m)(Q_{\text{obs}} - \bar{Q}_{\text{obs}})]^2}{\sum_{i=0}^{n} [(Q_{\text{obs}} - \bar{Q}_{\text{obs}})^2 \sum_{i=0}^{n} (Q_{\text{sim}} - \bar{Q}_{\text{sim}})^2]} \tag{4}$$

The RMSE observation standard deviation ratio (RSR) is a statistical metric that includes a scaling normalization factor and evaluates the relative performance of error indices RSR ranges from 0, which is the ideal value signifying zero RMSE, to a greater positive number:

$$\text{RSR} = \frac{\text{RMSE}}{\text{St. dev.} Q_{\text{obs}}} = \frac{\sqrt{(Q_{\text{obs}} - \bar{Q}_{\text{sim}})^2}}{\sqrt{(Q_{\text{obs}} - \bar{Q}_{\text{obs}})^2}} \tag{5}$$

The accuracy of the observed vs. simulated value plot's alignment with the 1:1 line is determined by the NSE simulation. The NSE is equal to 1 if the measured value agrees with all forecasts. The NSE indicates that there are discrepancies between the measured and anticipated values when it is between 0 and 1. Forecasts are particularly inaccurate when NSE is negative, and the average value of the output is a more accurate approximation than the model prediction. An NSE score of 1 indicates a perfect match between the simulated and observed data. The observed data mean is a better predictor than the simulated output when the NSE value is zero (Arnold *et al.* 2012):

$$\text{NSE} = \frac{\sum_{i=0}^{n} [(Q_{\text{obs}} - \bar{Q}_{\text{sim}})]^2}{\sum_{i=0}^{n} [(Q_{\text{obs}} - \bar{Q}_{\text{obs}})]^2} \tag{6}$$

The average tendency of simulated data to depart from their observed counterparts, either being higher or smaller, is quantified by the statistical term PBIAS. Zero is the ideal PBIAS value, which denotes a realistic and balanced model simulation. Greater precision is suggested by magnitude values that are lower. While negative PBIAS values signify an overestimation

bias in the model, positive values do the opposite:

$$\text{PBIAS} = \frac{\sum_{i=0}^{n} (Q_{\text{obs}} - \bar{Q}_{\text{sim}})}{\sum_{i=0}^{n} [(Q_{\text{obs}})]} \times 100 \tag{7}$$

where n is the total number of observations during the simulation period, Q_{obs} is observed flow data, Q_{sim} is the simulated value with respect to time, $\bar{Q}_{\text{sim}}$ and $\bar{Q}_{\text{obs}}$ are the arithmetic mean of simulated and observed data, respectively. The statistics suggested by Moriasi *et al.* (2007) served as the foundation for the model performance evaluations.

3. RESULTS AND DISCUSSION

3.1. Hydrological model performance

3.1.1. Sensitivity analysis, calibration, and validation

A set of 23 hydrological parameters were selected to identify the sensitive parameters for the calibration and validation of stream flow in the SWAT-CUP. The 23 parameters were run through a program with 500 simulations using the global sensitivity method to identify which ones were the most influential ones. The programme used a *t*-test and *p*-value to pinpoint the parameter that had a direct impact on the stream flow response. A *p*-value close to zero and a larger absolute value of the *t*-value indicates higher sensitivity of the parameter. Following the iterations, 12 parameters were identified as the most sensitive parameters (Table 2).

Curve number value (r_CN2.mng) followed by Plant Uptake Compensation factor (v_EPCO.hru) and Deep Aquifer Percolation fraction (v-RCHRG_DP.gw) are the top three most sensitive parameters.

Based on the results of the global sensitivity study, the 12 most sensitive parameters, listed in Table 2, were optimized using the SUFI2 algorithm in the SWAT-CUP. The majority of observed data is covered by the SUFI2 method, which includes all uncertainties and translates them onto parameter ranges to achieve a 95% prediction uncertainty. These uncertainties encompass various aspects such as model input, conceptualization, model parameters, and measured data (Abbaspour *et al.* 2004).

With a warm-up period of three years, calibration was carried out over a 13-year span, from 1 January 1990 to 31 December 2002 (Figure 4). Based on the calibration results of mean monthly stream flow, the SWAT model was able to replicate the observed streamflow. The statistical evaluation during the calibration period demonstrated a high level of agreement, as indicated by the R^2, NSE, PBIAS, and RSR values as shown in Table 3.

Table 2 | Sensitivity analysis and calibrated parameters

Parameter name	*t*-stat	Sensitivity *p*-value	Sensitivity rank	Calibration parameter value range	Fitted value
r_CN2.mng	−37.08	0.00	1	−20 to 20%	−1.02%
v_EPCO.bsn	−3.06	0.00	2	0–0.6	0.3
v_RCHRG-DP.gw	−2.72	0.00	3	0–0.6	0.47
v_EPCO.hru	2.19	0.02	4	0–0.2	0.17
v_ALPHA_BANK.rte	−1.88	0.05	5	0.2–0.78	0.59
a_GW_DELAY.gw	1.38	0.16	6	−10 to 10	−6
v_OV_N.hru	1.30	0.19	7	9–27	24.5
v_REVAPMN.gw	1.14	0.25	8	0–10	3.79
r_SOL_AWC (…)..sol	−1.07	0.28	9	−5 to 10%	2.46%
v_CANMAX.hru	1.04	0.29	10	0–6.4	5.55
v_CH_N2.rte	−1.03	0.30	11	0–0.4	0.3
v_GW_REVAP.gw	1.00	0.31	12	0–0.2	0.08

Note: v denotes replacing the parameter's original value, a denotes adding value to the initial parameter value, and r refers to multiplying the initial parameter value by its percent.

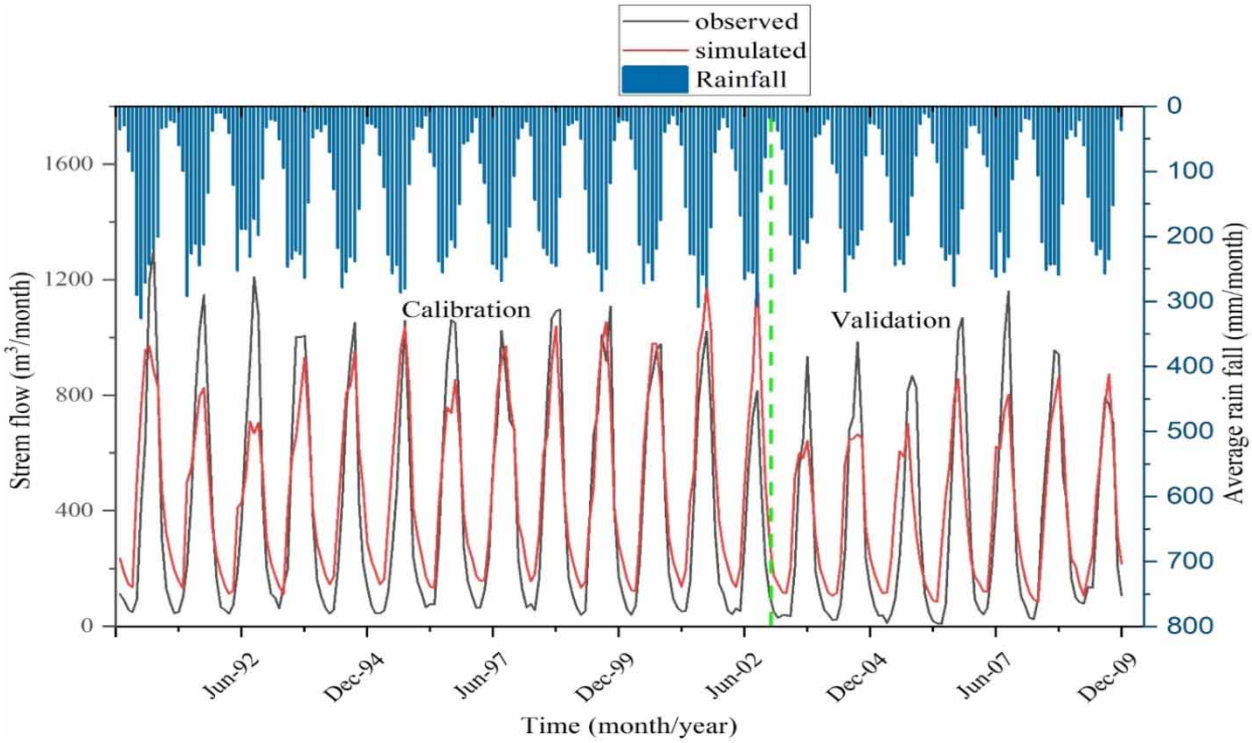

Figure 4 | Calibration and validation of average monthly stream flows.

Table 3 | Model calibration and validation performance

Criteria	Calibration	Validation
R^2	0.83	0.77
NSE	0.79	0.74
PBIAS	−15.2	−8.0
RSR	0.46	0.51

Model validation was carried out following model calibration. Model validation was done to determine how accurate the model was while replicating times that were not covered during calibration. By performing model validation, the suitability and reliability of the hydrological parameters derived during the calibration process were determined. For model validation, a 7-year period from 2003 to 2009 was analyzed. The average monthly flow validation results, shown in Table 3, include R^2, NSE, PBIAS, and RSR values.

This demonstrates that the validation outcomes for stream flow simulation with the SWAT model were satisfactory. Although the data used to evaluate the SWAT model during calibration and validation showed very good agreement between simulated and observed streamflow, the model was unable to reproduce peak flows in some of the years considered for calibration and validation. On the other hand, the SWAT model overestimated base flow in the majority of the calibration and validation periods considered. A similar case was reported by Dibaba *et al.* (2020), who noted that the SWAT model was unable to accurately simulate peak flow due to the second storm effect. In this study, we established a comprehensive model evaluation range for a monthly time step by incorporating performance ratings from the recommended statistics as proposed by Moriasi *et al.* (2007).

3.2. Impacts of climate change on hydrology

To assess the potential influence of climate change on the hydrological process of the basin, changes in temperature and rainfall patterns reported in Gebisa *et al.* (2023) were used. The projected temperature and rainfall values were used as inputs into the previously calibrated and validated SWAT model to simulate the impacts of climate change on the hydrological processes. The increase in the projected annual temperature and precipitation were found to have a substantial impact on the hydrological process of Baro River sub-basin under both SSP2-4.5 and SSP5-8.5. Even though the magnitude varied, both climate scenarios projected an increase in surface runoff, water yield, ET and PET and a decrease in groundwater. Table 4 shows that under the SSP2-4.5 scenario, there is an annual change of +100.43 mm (30.33%) in SURQ, −24.43 mm (−13.17%) in GWQ, +57.99 mm (6%) in WYLD, +34.8 mm (4.85%) in ET, and +45.1 mm (4.49%) in PET. Conversely, under the SSP5-8.5 scenario, the annual change shows +186.11 mm (44.67%) in SURQ, −5.39 mm (−2.64%) in GWQ, +199 mm (18.01%) in WYLD, +76.7 mm (10.1%) in ET, and +68.1 mm (6.63%) in PET. The findings regarding the impact of climate change on various hydrological processes are summarized in Table 4.

3.2.1. Impact of climate change on surface runoff and water yield

Changes in climate variables, particularly precipitation and temperature, have a substantial impact on surface runoff. As presented in Table 4, the projected annual runoff is expected to increase by +100.37 mm (30.33%) and +186.11 mm (44.67%) under SSP2-4.5 and SSP5-8.5, respectively, during 2031–2060. However, the increase in runoff varies across different seasons. In the JJA (June, July, August) and SON (September, October, November) seasons, the projected surface runoff is expected to rise by 25.48 and 43.7% under SSP2-4.5, and by 36.07 and 57.2% under SSP5-8.5, respectively. Similarly, the runoff in DJF (December, January, February) and MAM (March, April, May) seasons is projected to increase by 44.72 and 13.1% under SSP2-4.5, and by 80.22 and 43.41% under SSP5-8.5, respectively (Figure 5(a)). The increase in runoff during the dry season is beneficial for the region, especially since increased runoff during the wet season could lead to flooding. The correlation between surface runoff and precipitation is evident from the information presented in Table 4 and Figure 5(a). The fact that changes in precipitation directly affect the amount of surface runoff highlights the close connection between precipitation and surface runoff. This result is consistent with studies done in the Nile basin by Galata *et al.* (2021), where it was reported that an increase in projected precipitation led to a positive impact on surface runoff magnitude. Similar research was done by Demissie (2023) who reported that surface runoff exhibits an increase in the future projection. Furthermore, the study revealed that the percentage increase becomes more apparent under the RCP8.5 scenario in months where the estimated climate variables exhibit an increasing trend. Previous studies conducted in Ethiopia have reported an increase in stream flow within different catchments and basins (Getachew *et al.* 2021; Tessema *et al.* 2021). In the Kesem sub-basin, for instance, Tessema *et al.* (2021) reported an increase in mean annual flow, highlighting the significant role of large-scale sugar plantation irrigation downstream of the Kesem Dam.

In light of the implications of future climate change, it is projected that the overall water yield will increase both annually and seasonally as shown in Figure 5(b). The total annual water yield is projected to increase by +6 and +18% under SSP2-4.5 and SSP5-8.5, respectively. In the JJA and SON seasons, the projected water yield is expected to increase by 6.87 and 8.6% under SSP2-4.5, and by 16.3 and 20.01% under SSP5-8.5, respectively. Similarly, the water yield in the DJF and MAM seasons is projected to change by −4.63 and 0.1% under SSP2-4.5, and by 14.17 and 20.76% under SSP5-8.5, respectively. The

Table 4 | Mean annual hydrology of river basin under future climate scenario

Scenario		PCP	SURQ	LATQ	GWQ	WYLD	ET	PET
Baseline	1985–2014	1,666.2	230.56	207.41	209.87	908.49	682.4	959.3
SSP2-4.5	2031–2060	1,759.4	330.93	210.38	185.44	966.48	717.2	1,004.4
	Change (mm)	93.2	100.37	2.97	−24.43	57.99	34.8	45.10
	Change (%)	5.3	30.33	1.41	−13.17	6.0	4.85	4.49
SSP5-8.5	2031–2060	1,945.7	416.67	228.57	204.48	1,108.09	759.1	1,027.4
	Change (mm)	279.5	186.11	21.16	−5.39	199.6	76.7	68.1
	Change (%)	14.4	44.67	9.26	−2.64	18.01	10.10	6.63

PCP, precipitation; SURQ, surface runoff; LATQ, lateral flow into the stream; WYLD, total water yield; GWQ, groundwater contribution to stream flow; ET, actual evapotranspiration; PET, potential evapotranspiration.

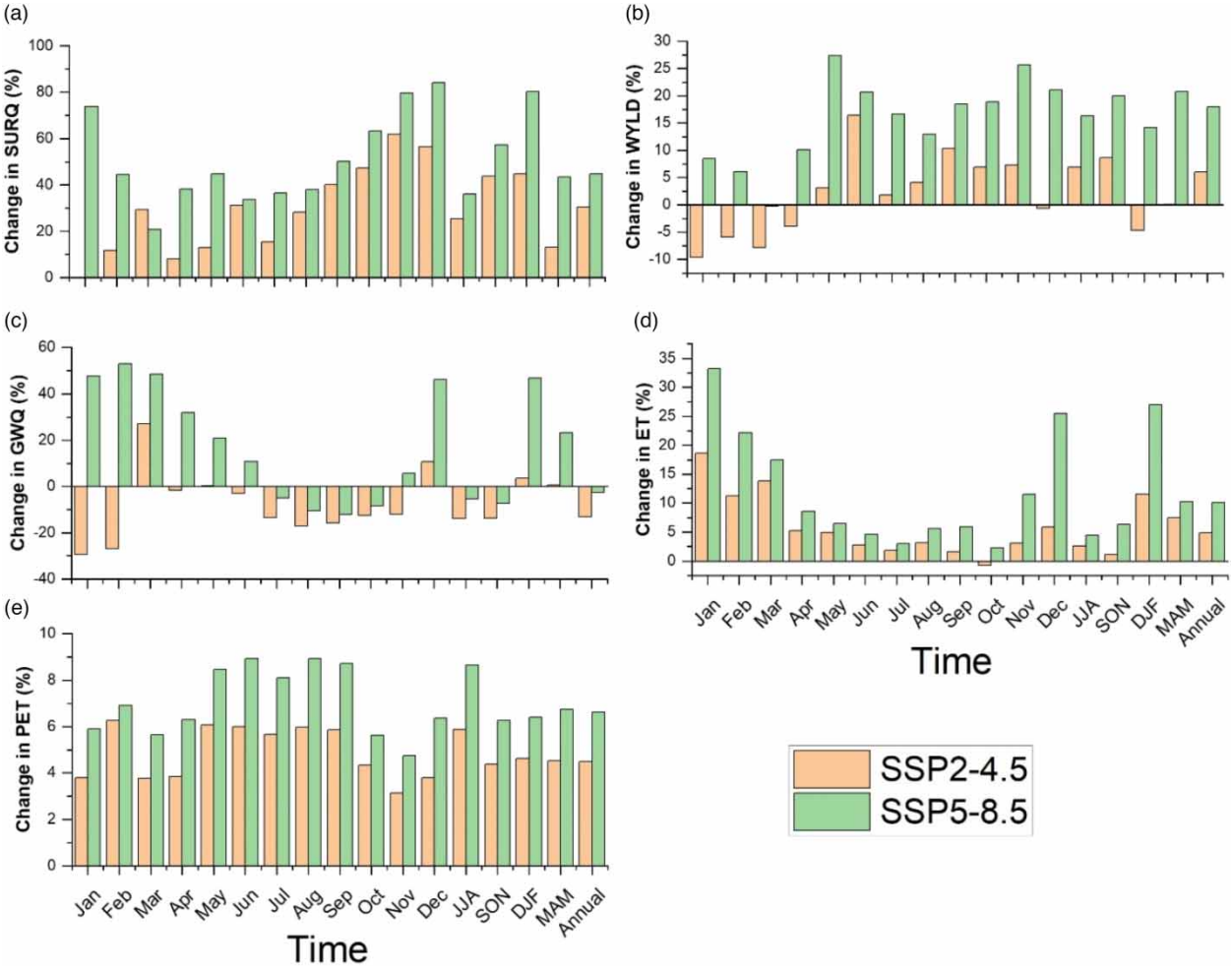

Figure 5 | Change in mean monthly, seasonal, and annual surface runoff (a), water yield (b), groundwater (c), evapotranspiration (d), and potential evapotranspiration (e) for the future period (2031–2060) under SSP2-4.5 and SSP5-8.5.

projected precipitation under SSP5-8.5 is greater than under SSP2-4.5. Consequently, the water yield during the SON season under SSP5-8.5 is almost similar to the water yield during the MAM season under SSP5-8.5. Therefore, the change in precipitation is the most significant factor influencing these variables. The total water yields are impacted by elements including surface runoff, groundwater flow, and water loss reduction when groundwater flow drops in particular months. The expected increase in rainfall and streamflow could have a number of outcomes. On the one hand, it might offer an abundance of water resources to support the basin's expanding population. While a decrease in rainfall during the minor rainy season increases the likelihood of water scarcity and stress, projections for increased rainfall during the major rainy season raise concerns about a heightened risk of flooding. This study closely resembles the work of Tessema *et al.* (2021) conducted in the Kesem sub-basin and similar areas in Ethiopia, providing valuable insights to support current and future water resource management in the Baro River sub-basin. In a comparable scenario, this study exhibits similarities with the research conducted by Wagena *et al.* (2016), emphasizing both the significant variability in climate change impacts and the potential for positive outcomes in the region.

3.2.2. Impact of climate change on ground water hydrology

The projection of seasonal and annual groundwater (GWQ) showed a decreasing trend under both SSP2-4.5 and SSP5-8.5 scenarios. The annual projected GWQ decline under SSP2-4.5 and SSP5-8.5 scenarios showed a decrease by 13.17 and 2.64%, respectively (Figure 5(c)). Although the decrease in GWQ with rising precipitation may seem contradictory, increased

SURQ with higher precipitation may reduce GWQ recharge depending on soil conditions. Furthermore, larger increases in temperature and PET may result in higher rates of ET which contributes to the high rate of water loss. This could lower the amount of accessible water for GWQ recharge. Consequently, the increase in surface runoff and decrease in infiltration could lead to a reduction in groundwater. This finding is consistent with the study by Tigabu *et al.* (2021), who reported that increased runoff, along with reduced infiltration, led to reduced groundwater.

While the direct measurement of temperature's impact on groundwater may be challenging, it can be deduced from other hydrological factors such as ET. On the other hand, one of the factors contributing to the decrease in groundwater is soil moisture dynamics. Increased temperatures can alter these dynamics, leading to drier soils, which in turn can reduce the infiltration rates of precipitation into the ground and hence lower groundwater recharge (Vereecken *et al.* 2008). Positive or negative changes in one hydrological component might have an impact on other components in the system. Although temperature does not directly affect ET, it does have an impact on PET. However, the actual ET also depends on the availability of water, which can be limited, particularly during certain seasons. Additionally, higher rainfall intensity exacerbates the situation by promoting rapid overland flow and reduced infiltration. While overall precipitation may increase, changes in its distribution, intensity, and frequency can impact groundwater recharge. More frequent heavy rains can result in increased surface runoff, which does not effectively infiltrate the ground (Vereecken *et al.* 2008). Similar findings related to the impacts of climate change have been reported in different parts of Ethiopia (Mengistu *et al.* 2020; Tigabu *et al.* 2021). According to Tigabu *et al.* (2021), the projected decline in groundwater flow was reported along with an increase in surface runoff in Lake Tana. Mengistu *et al.* (2020), on the other hand, found that the total water yield of the Upper Blue Nile basin was projected to decrease despite the increase in surface runoff. In future scenarios, higher temperatures and changing precipitation patterns may increase water demand for agricultural, industrial, and domestic uses. This could lead to higher rates of groundwater extraction, further depleting groundwater reserves in the river basin.

3.2.3. Impact of climate change on ET and PET

PET and actual ET can be influenced by the projected changes in temperature and precipitation. As a result, a rise in temperature may cause ET and evaporation rates to increase, which could hasten the depletion of groundwater supplies. Figure 5(e) shows that annual PET was increased by +4.49 and +6.63% under SSP2-4.5 and SSP5-8.5, respectively.

The annual ET was increased by +4.85 and +10.1% under SSP2-4.5 and SSP5-8.5, respectively, as shown by Figure 5(d). The rise in PET and ET is more pronounced under SSP5-8.5 compared to SSP2-4.5, due to the higher temperature change associated with SSP5-8.5. ET is a vital component of the hydrological cycle. It is crucial to account for this natural process when assessing agricultural water demand and determining the practical storage capacity of a dam (Adib *et al.* 2023). The current study shows an increase in annual PET across all periods and SSPs, possibly due to a rise in temperature. Similarly, ET is expected to increase alongside a rising temperature, although this is limited by water availability. The increase in ET during JJA is 2.61% under SSP2-4.5 and 4.43% under SSP5-8.5, while in DJF, ET increases by 11.55 and 27.02% under SSP2-4.5 and SSP5-8.5, respectively. ET is greater during the dry season than the wet season as shown in Figure 5(d). The results are consistent with the findings of various researchers in Ethiopia (Daba & Nageswara 2016; Seneshaw *et al.* 2020). For instance, Seneshaw *et al.* (2020) reported that ET is projected to rise under all scenarios as temperatures increases. Another study in the Upper Blue Nile basin showed that higher precipitation and a rising temperature contributed to an increase in evaporation (Getachew *et al.* 2021). Overall, the interaction between precipitation, temperature, and ET serves to illustrate the impact of climate change on a basin's hydrology. An increase in precipitation amplifies surface runoff, while a rise in temperature leads to increased PET and decreased groundwater levels within the hydrological system.

3.3. Spatial distribution of hydrological process

Although the impacts of climate change is projected to increase surface runoff, water yield, and ET, while decreasing groundwater in the Baro River sub-basin, each sub-basin exhibits distinct yield characteristics. While precipitation changes have direct impact on the hydrological process, changes in temperature are predicted to have an indirect impact.

The most substantial increases in surface runoff and water yield are projected in the northern and southern regions of the basin under both SSP2-4.5 and SSP5-8.5 as shown in Figure 6. The highest increase in surface runoff in the southern part is attributed by the highest increase in the projected precipitation as presented by Gebisa *et al.* (2023). The southern part of the river basin is also the area with the highest elevation. The projection shows a greater increase in surface runoff and water yield under SSP5-8.5 compared to SSP2-4.5. Conversely, the lowest increase in surface runoff is projected in the northwest

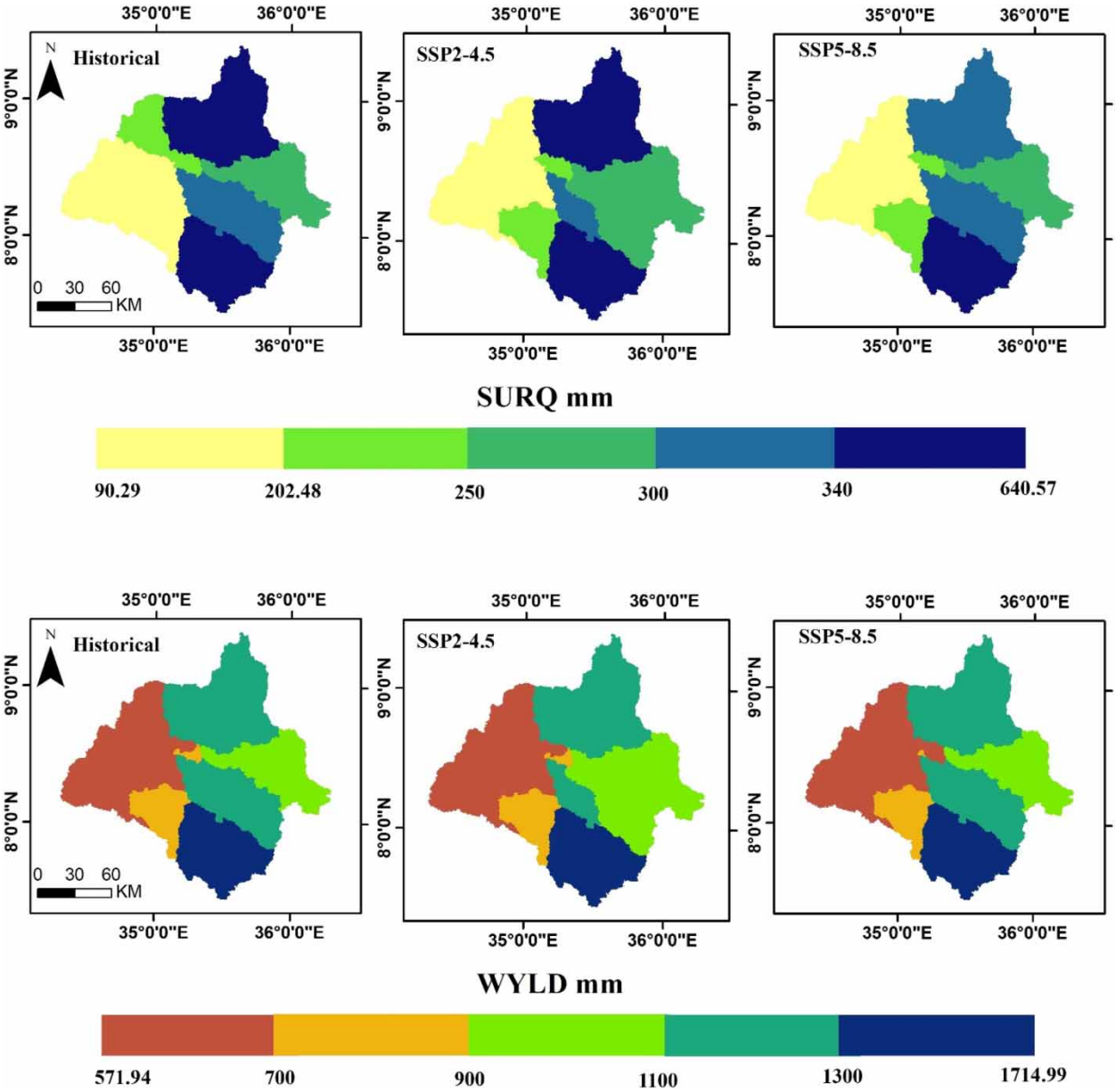

Figure 6 | Mean annual surface runoff (SURQ) and water yield (WYLD) under the baseline (1985–2014) and future (2031–2060) climate scenario in each sub-watershed of the Baro River sub-basin.

and southeast areas, with a slight increase observed downstream. The northwest part of the region is also characterized with the lowest increase in projected precipitation. The smallest decrease in water yield is projected in the southeastern region under SSP2-4.5, while the lowest increase is expected in the central northwest under SSP5-8.5.

Figure 7 shows the spatial distribution of groundwater and ET under the projected climate change for both SSP2-4.5 and SSP5-8.5 scenarios. The smallest increase was projected in the northern part under SSP2-4.5 and in the western part under SSP5-8.5. The areas covered by vegetation around the southern parts resulted in low surface runoff and high groundwater recharge. On the other hand, the areas dominated by agriculture around the northern parts shows high surface runoff and lower groundwater.

The highest rise in ET is shown by SSP2-4.5 around the south and northwest of the basin, while south and the east of the basin was projected under SSP5-8.5. The lowest increase was projected around the north under SSP2-4.5 and in the west

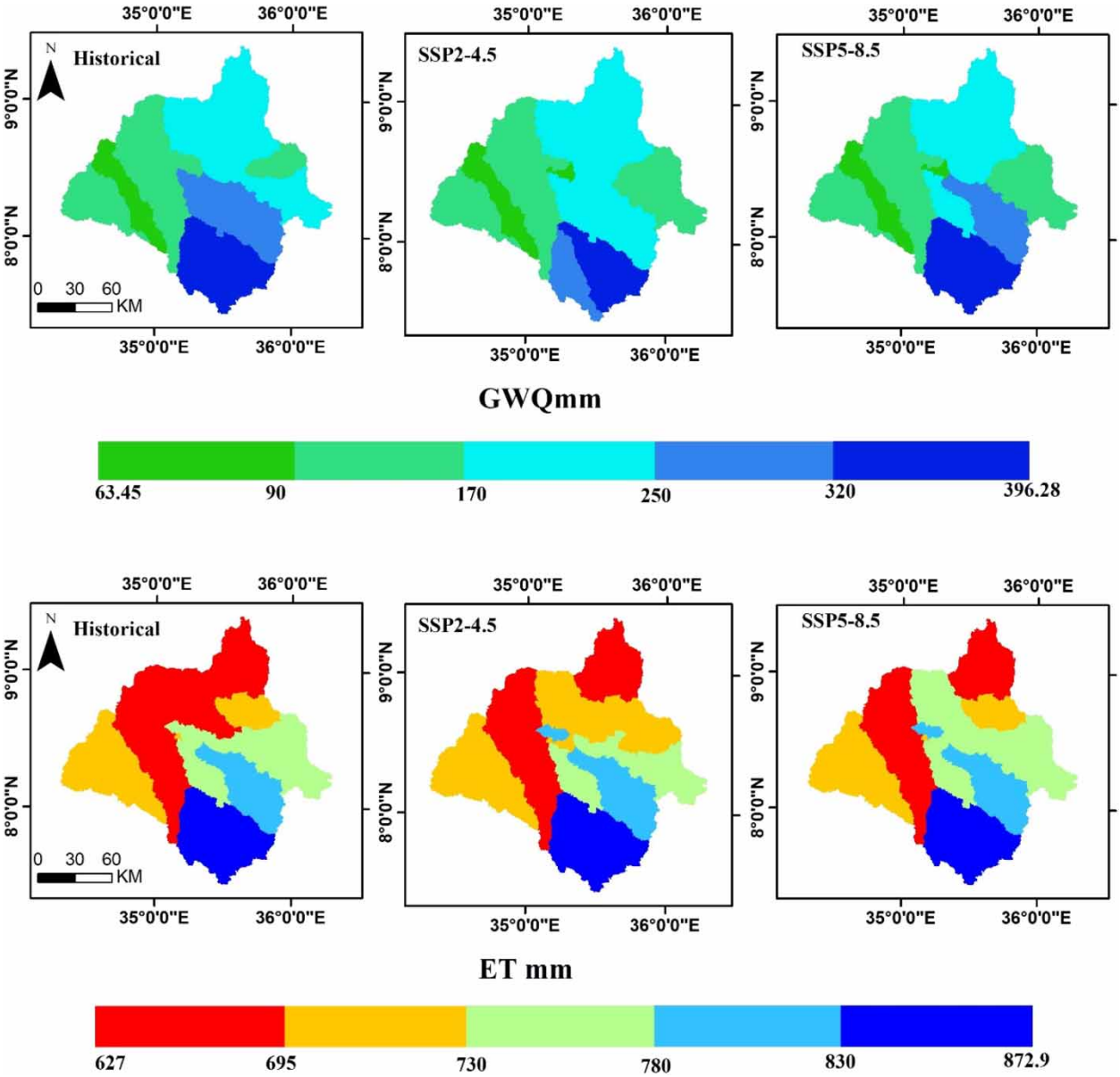

Figure 7 | Mean annual ground water (GWQ) and ET under the baseline (1985–2014) and future (2031–2060) climate scenario in each sub-watershed of the Baro River sub-basin.

under SSP5-8.5. In the projected climatic change for this study, ET increased at a higher rate under SSP5-8.5 than under SSP2-4.5. The projected future climate was marked by higher rates of evaporation and more seasonal water loss, which affects the groundwater and water yield. This is in agreement with previous studies. Earlier studies show that the ET increases (Ungtae & Kaluarachchi 2009; Dibaba *et al.* 2020). The study by Dibaba *et al.* (2020) reported that the increase in ET was higher under RCP8.5 compared to RCP4.5. The expected temperature rises in future climate scenarios are probably what caused the observed hydrological alterations.

Overall, this study assessed the effects of anticipated climate change, assuming constant LULC for both historical and future periods. When examining future scenarios, essential weather variables such as solar radiation, relative humidity, and wind speed from the historical period were held constant without modification. It is crucial to note that in reality, variations in these weather variables and alterations in LULC occur due to both natural processes and human activities. Consequently, a more comprehensive understanding can be achieved by conducting research that considers changes in these weather variables and LULC, thereby enhancing the reliability of the study's findings.

4. CONCLUSION

Following an evaluation of the model performances of the global climate models (GCMs), which are components of CMP6, this paper evaluated the ensemble modeling of the hydrological impacts of climate change on the Baro River sub-basin. For the analysis of the climate change impacts, GFDL-CM4, INM-CM5-0, and INM-CM4-8 were used for precipitation and minimum temperature while CMCC-ESM2, MRI-ESM2-0, and INM-CM4-8 were used for maximum temperature.

The study demonstrated the significance of using the models that are perceived as atypical or least realistic in a given study region in order to reduce the uncertainty associated with the individual GCMs. Consequently, the multi-mean ensemble of three GCMs was employed in the study after the representative models had been determined based on spatial, seasonal, and multivariate statistics. Using a bias-corrected ensemble of the GCMs, the hydrology impacts of climate change were conducted with a calibrated and validated SWAT model. Although the SWAT model was capable of simulating the rising and recession limbs of the hydrographs, it was unable to simulate the peak flow. The results of the ensemble GCMs showed an increasing precipitation and temperature under both climate scenarios used in this study. Consequently, annual and seasonal surface runoff is projected to increase under both SSPs. The increasing surface runoff is related to the increase in precipitation. Contrarily, the annual decrease in groundwater flow (GWQ) was evident under SSP2-4.5 and SSP5-8.5 scenarios. Both ET and PET were increased, and raising PET resulted in a decrease in soil moisture due to rising temperatures.

The special distribution of the hydrological process under the climate change shows that the projected increase in surface runoff and water yield is highest in the northern and southern parts of the basin, under both SSP2-4.5 and SSP5-8.5 scenarios. Groundwater decline is significantly more pronounced in the southeast under both SSP scenarios.

The study finding provided crucial details on the relative influences on how the hydrological process responds to climate change scenarios. This is an important contribution as it could help to plan proper water resources management interventions. The outcome emphasises the necessity of regional cooperation and development to promote effective management techniques that are climate resilient and to slow down the study area's accelerating climate change.

ACKNOWLEDGEMENTS

The authors express their gratitude to Bule Hora University and Jimma University for hosting and supporting the study. We would especially like to acknowledge the Ethiopian National Meteorological Agency for providing the data on the observed climate and the Ministry of Water and Energy for providing the data on the observed stream flow. Additionally, the authors extend their appreciation to the Working Groups of the World Climate Research Program for making CMIP6 available in the Earth System Federation (ESGF) Archive.

FUNDING

The authors confirm that they did not receive any funds, grants, or other support during the preparation of this manuscript.

DATA AVAILABILITY STATEMENT

Data cannot be made publicly available; readers should contact the corresponding author for details.

CONFLICT OF INTEREST

The authors declare there is no conflict.

REFERENCES

Abbaspour, K. C., Johnson, C. A. & van Genuchten, M. T. (2004) Estimating uncertain flow and transport parameters using a sequential uncertainty fitting procedure, *Vadose Zone Journal*, **3** (4), 1340–1352. https://doi.org/10.2136/vzj2004.1340.

Adib, A., Kalantarzadeh, S. S. O., Shoushtari, M. M., Lotfirad, M., Liaghat, A. & Oulapour, M. (2023) Sensitive analysis of meteorological data and selecting appropriate machine learning model for estimation of reference evapotranspiration, *Applied Water Science*, **13** (3), 1–17. https://doi.org/10.1007/s13201-023-01895-5.

Arnell, N. W. (2003) Effects of IPCC SRES emissions scenarios on river runoff: A global perspective, *Hydrology and Earth System Sciences*, **7** (5), 619–641. https://doi.org/10.5194/hess-7-619-2003.

Arnold, J. G. & Fohrer, N. (2005) SWAT2000:Current capabilities and research opportunities in applied watershed modeling, *Hydrological Processes*, **19**, 563–572. https://doi.org/10.1002/hyp.5611.

Arnold, J. G., Moriasi, D. N., Gassman, P. W. & White, M. J. (2012) SWAT : Model use, calibration, and validation, *Biological System Engineering*, **55**, 1491–1508.

Beyene, T., Lettenmaier, D. P. & Kabat, P. (2010) Hydrologic impacts of climate change on the Nile River Basin: Implications of the 2007 IPCC scenarios, *Climatic Change*, **100** (3), 433–461. https://doi.org/10.1007/s10584-009-9693-0.

Bodian, A., Dezetter, A., Diop, L., Deme, A., Djaman, K. & Diop, A. (2018) Future climate change impacts on streamflows of two main West Africa river basins: Senegal and Gambia, *Hydrology*, 1–18. https://doi.org/10.3390/hydrology5010021.

Chaemiso, S. E., Abebe, A. & Pingale, S. M. (2016) Assessment of the impact of climate change on surface hydrological processes using SWAT: A case study of Omo-Gibe river basin, Ethiopia, *Modeling Earth Systems and Environment*, **2** (4), 1–15. https://doi.org/10.1007/s40808-016-0257-9.

Chen, Y., Li, Z., Fan, Y., Wang, H. & Deng, H. (2015) Progress and prospects of climate change impact on hydrology in the arid region of northwest China, *Environmental Research*, 1–9. https://doi.org/10.1016/j.envres.2014.12.029.

Coulibaly, N., Honoré, C. J., Mpakama, Z. & Savané, I. (2018) The impact of climate change on water resource availability in a trans-boundary basin in West Africa, *Hydrology*, **1**, 13. https://doi.org/10.3390/hydrology5010012.

Daba, M. & Nageswara, R. G. (2016) Evaluating potential impacts of climate change on hydro- meteorological variables in upper blue Nile basin, Ethiopia a case study of finchaa sub-basin, *Environment and Earth Science*, **6**, 48–57.

Demissie, T. A. (2023) Impact of climate change on hydrologic components using CORDEX Africa climate model in Gilgel Gibe 1 watershed Ethiopia, *Heliyon*, **9** (6), e16701. https://doi.org/10.1016/j.heliyon.2023.e16701.

Dibaba, W. T., Demissie, T. A. & Miegel, K. (2020) Watershed hydrological response to combined land use/land cover and climate change in highland Ethiopia: Finchaa catchment, *Water*. https://doi.org/10.3390/w12061801.

Galata, A. W., Tullu, K. T. & Guder, A. C. (2021) Evaluating watershed hydrological responses to climate changes at Hangar Watershed, Ethiopia, *Water and Climate Change*, 2271–2287. https://doi.org/10.2166/wcc.2021.229.

Gebisa, B. T., Dibaba, W. T. & Kabeta, A. (2023) Evaluation of historical CMIP6 model simulations and future climate change projections in the Baro River Basin, *Water and Climate Change*, **14**, 1–26. https://doi.org/10.2166/wcc.2023.032.

Gelete, G., Gokcekus, H. & Gichamo, T. (2020) Impact of climate change on the hydrology of Blue Nile basin, Ethiopia: A review, *Water and Climate Change*, **11** (4), 1–12. https://doi.org/10.2166/wcc.2019.014.

Getachew, B., Manjunatha, B. R. & Bhat, H. G. (2021) Modeling projected impacts of climate and land use/land cover changes on hydrological responses in the Lake Tana Basin, upper Blue Nile River Basin, Ethiopia, *Journal of Hydrology*, **595**, 1–20. https://doi.org/10.1016/j.jhydrol.2021.125974.

Haerter, J. O., Hagemann, S., Moseley, C. & Piani, C. (2011) Climate model bias correction and the role of timescales, *Hydrology and Earth System Sciences*, **15** (3), 1065–1079. https://doi.org/10.5194/hess-15-1065-2011.

IPCC (2013) Climate Change 2013: The Physical Science Basis. In: Stocker, T. F., Qin, D., Plattner, G.-K., Tignor, M., Allen, S. K., Boschung, J., Nauels, A., Xia, Y., Bex, V. & Midgley, P. M. eds., *Contribution of Working Group I to the Fifth Assessment Report of the Intergovernmental Panel on Climate Change*. Cambridge University Press, Cambridge, United Kingdom and New York, NY, USA, 1535 pp.

IPCC (2014) *Climate Change 2014: Synthesis Report. Contribution of Working Groups I, II and III to the Fifth Assessment Report of the Intergovernmental Panel on Climate Change*. Geneva, Switzerland: IPCC.

Khatun, S., Sahana, M., Jain, S. K. & Jain, N. (2018) Simulation of surface runoff using semi-distributed hydrological model for a part of Satluj Basin: Parameterization and global sensitivity analysis using SWAT CUP, *Modeling Earth Systems and Environment*, **4** (3), 1111–1124. https://doi.org/10.1007/s40808-018-0474-5.

Mengistu, D., Bewket, W., Dosio, A. & Panitz, H. (2020) Climate change impacts on water resources in the Upper Blue Nile (Abay) River Basin, Ethiopia, *Journal of Hydrology*, 1–44. https://doi.org/10.1016/j.jhydrol.2020.125614.

Mengistu, A. G., Woldesenbet, T. A., Dile, Y. T., Bayabil, H. K. & Tefera, G. W. (2023) Modeling impacts of projected land use and climate changes on the water balance in the Baro basin, Ethiopia, *Heliyon*, **9** (3), e13965. https://doi.org/10.1016/j.heliyon.2023.e13965.

Moriasi, D. N., Arnold, J. G., Van Liew, M. W., Bingner, R. L., Harmel, R. D. & Veith, T. L. (2007) Model evaluation guidelines for systematic quantification of accuracy in watershed simulations, *American Society of Agricultural and Biological Engineers*, **50** (3), 885–900.

Muleta, T. N. (2021) Climate change scenario analysis for Baro - Akobo river basin, Southwestern Ethiopia, *Environmental Systems Research*, 1–15. https://doi.org/10.1186/s40068-021-00225-5.

Neitsch, S. L., Arnold, J. G., Kiniry, J. R. & Williams, J. R. (2005) *Soil & Water Assessment Tool Theoretical Documentation Version 2005*. Temple, YX: Soil and Water Research Laboratory, Agricultural Research Service. US Department of Agriculture. Available at: https://swat.tamu.edu/media/1292/swat2005theory.pdf.

Neitsch, S. L., Arnold, J. G., Kiniry, J. R. & Williams, J. R. (2011) *Soil and Water Assessment Tool Theoretical Documentation version 2009*, Temple, TX: Water Research Institute, College Station, TX, USA. https://swat.tamu.edu/media/99192/swat2009-theory.pdf.

NMA (2007) Climate Change National Adaptation Programme of Action (NAPA) of Ethiopia. Addis Ababa, Ethiopia: National Meteorological Agency.

Pierce, D. W., Cayan, D. R., Maurer, E. P., Abatzoglou, J. T. & Hegewisch, K. C. (2015) Improved bias correction techniques for hydrological simulations of climate change, *Journal of Hydrometeorology*, **16** (6), 2421–2442. https://doi.org/10.1175/JHM-D-14-0236.1.

Roth, V., Lemann, T., Zeleke, G. & Teklay, A. (2018) Effects of climate change on water resources in the upper Blue Nile Basin of Ethiopia, *Heliyon*, 1–28. https://doi.org/10.1016/j.heliyon.2018.e00771.

Saharia, A. M. & Sarma, A. K. (2018) Future climate change impact evaluation on hydrologic processes in the Bharalu and Basistha basins using SWAT model, *Natural Hazards*, **92** (3), 1463–1488. https://doi.org/10.1007/s11069-018-3259-2.

Sao, D., Kato, T., Tu, L. H., Thouk, P., Fitriyah, A. & Oeurng, C. (2020) Evaluation of different objective functions used in the SUFI-2 calibration process of SWAT-CUP on water balance analysis: A case study of the pursat, *Water*, **12**. https://doi.org/10.3390/w12102901.

Seneshaw, G. Y., Hsu, L. M. & Yuan, C. P. (2020) Assessing the impact of climate change on the hydrology of Melka Kuntrie Subbasin, Ethiopia with Ar4 and Ar5 projections, *Water*, **12** (5). https://doi.org/10.3390/W12051308.

Setegn, S. G., Rayner, D., Melesse, A. M., Dargahi, B. & Srinivasan, R. (2011) Impact of climate change on the hydroclimatology of Lake Tana Basin, Ethiopia, *Water Resources Research*, **47** (4), 1–13. https://doi.org/10.1029/2010WR009248.

Taye, M. T., Dyer, E., Hirpa, F. A. & Charles, K. (2018) Climate change impact on water resources in the Awash basin, Ethiopia, *Water (Switzerland)*, **10** (11), 1–16. https://doi.org/10.3390/w10111560.

Tessema, N., Kebede, A. & Yadeta, D. (2021) Modelling the effects of climate change on streamflow using climate and hydrological models: The case of the Kesem sub-basin of the Awash River basin, Ethiopia, *International Journal of River Basin Management*, **19** (4), 469–480. https://doi.org/10.1080/15715124.2020.1755301.

Tigabu, T. B., Wagner, P. D., Hörmann, G., Kiesel, J. & Fohrer, N. (2021) Climate change impacts on the water and groundwater resources of the lake tana basin, Ethiopia, *Journal of Water and Climate Change*, **12** (5), 1544–1563. https://doi.org/10.2166/wcc.2020.126.

Ungtae, K. & Kaluarachchi, J. J. (2009) Climate change impacts on water resources in the upper Blue Nile River Basin, Ethiopia, *Journal of the American Water Resources Association*, **45** (6), 1361–1378. https://doi.org/10.1111/j.1752-1688.2009.00369.x.

Vereecken, H., Huisman, J. A., Bogena, H., Vanderborght, J., Vrugt, J. A. & Hopmans, J. W. (2008) On the value of soil moisture measurements in vadose zone hydrology: A review, *Water Resources Research*, **44** (4), 1–21. https://doi.org/10.1029/2008WR006829.

Wagena, M. B., Sommerlot, A., Abiy, A. Z., Collick, A. S., Langan, S., Fuka, D. R. & Easton, Z. M. (2016) Climate change in the Blue Nile Basin Ethiopia: Implications for water resources and sediment transport, *Climatic Change*, 229–243. https://doi.org/10.1007/s10584-016-1785-z.

Worku, G., Teferi, E., Bantider, A. & Dile, Y. T. (2021) Climate Risk Management Modelling hydrological processes under climate change scenarios in the Jemma sub-basin of upper Blue Nile Basin, Ethiopia, *Climate Risk Management*, **31**, 1–20. https://doi.org/10.1016/j.crm.2021.100272.

First received 6 May 2024; accepted in revised form 28 October 2024. Available online 6 November 2024